HHS Public Access

Author manuscript

ACS Appl Mater Interfaces. Author manuscript; available in PMC 2021 December 17.

Published in final edited form as:

ACS Appl Mater Interfaces. 2017 November 22; 9(46): 40671–40680. doi:10.1021/acsami.7b12734.

Nanozyme-Mediated Dual Immunoassay Integrated with Smartphone for Use in Simultaneous Detection of Pathogens

Nan Cheng[†,§,‖], **Yang Song**[†], **Mohamed M. A. Zeinhom**[†,⊥], **Yu-Chung Chang**[†], **Lina Sheng**[‡], **Haolin Li**[‖], **Dan Du**[†], **Lei Li**[†], **Mei-Jun Zhu**[‡], **Yunbo Luo**[§,‖], **Wentao Xu**[*,§,‖], **Yuehe Lin**[*,†]

[†]School of Mechanical and Materials Engineering, Washington State University, Pullman, Washington 99164, United States

[‡]School of Food Science, Washington State University, Pullman, Washington 99164, United States

[§]Beijing Advanced Innovation Center for Food Nutrition and Human Health, College of Food Science & Nutritional Engineering, China Agricultural University, Beijing 100083, China

[‖]Beijing Laboratory for Food Quality and Safety, College of Food Science and Nutritional Engineering, China Agricultural University, Beijing 100083, China

[⊥]Food Hygiene Department, Faculty of Veterinary Medicine, Beni-Suef University, Beni-Suef 62512, Egypt

Abstract

Nanozymes are an excellent class of optical reporters for the development of sensitive biosensors for widespread applications. In this study, mesoporous core–shell palladium@platinum (Pd@Pt) nanoparticles were synthesized and then applied as signal amplifier in a dual lateral flow immunoassay (LFIA) and integrated with a smartphone-based device for use in simultaneous detection of *Salmonella* Enteritidis and *Escherichia coli* O157:H7. After optimization, the limit of detections were calculated to be ~20 cfu/mL for *S.* Enteritidis and ~34 cfu/mL for *E. coli* O157:H7, respectively. The greatly improved sensitivity was contributed by the peroxidase-like catalytic activity of the Pd@Pt nanoparticles for signal enhancement and the parallel design of dual detection for eliminating the cross-interference. The estimated recoveries of the dual LFIA range from 91.44 to 117.00%, which indicated that the developed method is capable of detecting live bacteria in food samples. This approach provides an attractive platform for *S.* Enteritidis and *E. coli* O157:H7 detection using a smartphone-based device as the sole piece of equipment, indicating great promise for foodborne pathogen analysis or infield food safety tracking.

Graphical Abstract

[*]**Corresponding Authors** xuwentao@cau.edu.cn (W.X). yuehe.lin@wsu.edu (Y.L).

The authors declare no competing financial interest.

ASSOCIATED CONTENT

Supporting Information

The Supporting Information is available free of charge on the ACS Publications website at DOI: 10.1021/acsami.7b12734.

Additional details regarding characterization of nanoparticles by means of ζ potential and FTIR spectra, different conditions of blue signals on the lines, catalytic function of nanoparticles, and specificity test images (PDF)

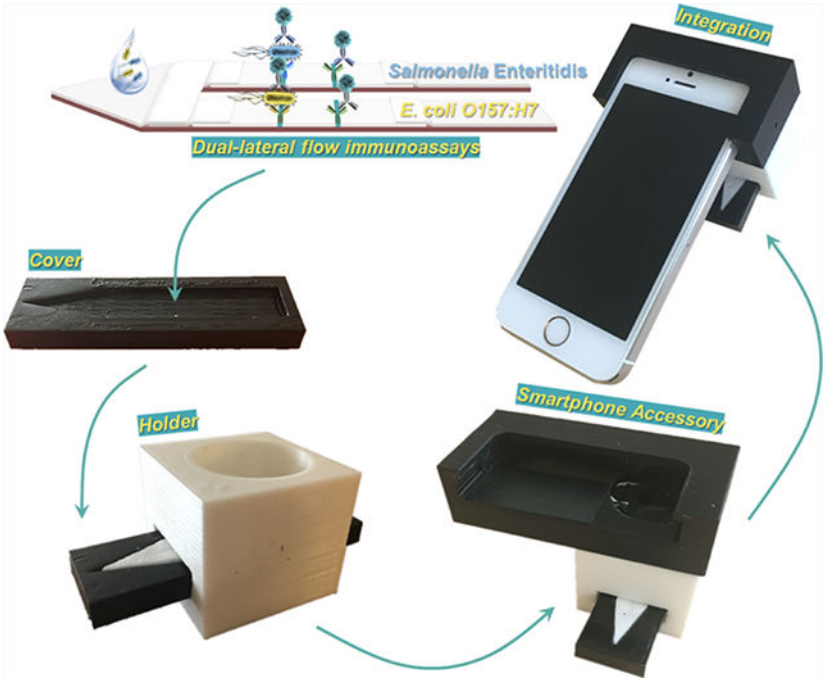

Keywords

lateral flow immunoassay; Pt–Pd nanoparticles; milk; Salmonella Enteritidis; E. coli O157:H7; smartphone

1. INTRODUCTION

Nanozymes are an excellent class of optical reporters for the development of sensitive biosensors for broad applications,[1–4] which could significantly improve the sensitivity and lower the limit of detection (LOD) of biosensors because they can retain the original color properties and provide other stronger colors through catalysis.[5] Platinum–palladium (Pd–Pt) nanoparticles, an attractive class of nanozymes with two components, are potential candidates as signal amplification because of the cooperative interactions result in important features, including enhanced peroxidase-like catalytic activity, increased surface area, and increased robustness.[6,7] The superiority of Pd–Pt nanoparticles makes them highly desirable for detection of pathogens, which are still a major public health threat to countries all around the world.[8] According to the Center for Disease Control (CDC), pathogens caused about 112 000 disability-adjusted life years (DALYs) annually in the United States.[9] The rates of DALYs were higher in the Middle Eastern and African regions.[10] Among foodborne pathogens, *Salmonella* and *Escherichia coli* O157:H7 are the most common causes of the recent outbreaks and hospitalizations problems that affect millions of people annually.[11,12] Therefore, the determination of the two pathogens in a single powerful analytical tool would be of a great value to food safety and human health.

The current gold standard for viable bacterial detection is the culture method, which requires a number of serological and biochemical tests and takes several days to confirm

a certain bacterium.[13] To overcome the obstacles of single-targeting, labor-intensive and time-consuming method, and informational delay, nonculture methods have been developed on the basis of the principles of biometric elements, such as nucleic acid and antibody.[14] Nucleic acid-based techniques, the gold standard for total bacterial detection, could be multiplexed, sensitive, and specific but often require expensive instruments and skilled technical staff, which may have limited suitability for developing regions.[15] Alternatively, immunoassays, such as gold nanoparticle (AuNP)-based lateral flow immunoassays (LFIAs), have been developed to address these issues because of their instrument-free, low-cost, easy-operating, and rapid detection.[16,17] Although promising, their application is greatly limited due to the LOD of reported AuNP-based LFIAs. Magnetic beads were used to preconcentrate cells and improve sensitivity, but they included additional operating procedures and increased assay time.[18–20] Horseradish peroxidase (HRP)-enhanced LFIAs were also published to improve sensitivity, but they need additional modification of HRP, which increased the cost and limited their shelf life due to the gradual loss of enzyme activity. Moreover, the detection ability of more than one biomarker in a single LFIA at once is emerging in response to bacteria. Some multi-LFIAs have already been reported and applied for simultaneous analysis of different bacteria.[21,22] However, simply adding more test lines may not be encouraged because of unexpected cross-reaction, enlarged assay time, and erratic nanomaterial distribution.[23,24] Another limitation is that specific quantitative readers may not be appropriate for the food industry, which deals with high consumer demand and timely epidemic outbreak prevention.[25] Hence, it is still an incremental challenge to develop a sensitive nanoparticle-based assay and portable quantitative device.

To provide a portable and cost-effective platform to record results, smartphone-based device can be considered as one of the most attractive candidates for the development of point-of-care (POC) diagnostics platforms.[26] By the end of 2015, the smartphone penetration rate in North America, Europe, and Africa was estimated to be more than 60, 45, and 25%, respectively.[27] Moreover, the device can be made with low-cost 3D printing technology and be exploited to perform analysis infield using simple procedures.[28] Recent papers showed that it is possible to use a smartphone as a detector for a single LFIA,[29–31] which decreases costs and increases healthcare availability and accessibility. To the best of our knowledge, dual LFIA has not yet been implemented using a smartphone-based device.

In this work, nanozyme was applied as signal amplifier in a dual LFIA and integrated with a smartphone-based device for use in simultaneous detection of *Salmonella* Enteritidis and *E. coli* O157:H7. The system features three main components: (1) nanozyme (mesoporous Pd@Pt nanoparticles) instead of AuNPs or HRP as signal amplification for their abilities of improving the sensitivity and stability; (2) dual LFIA for its ability of simultaneous detection of targets exhibiting attractive features, including real time, easy-to-use, and high-specificity; and (3) a smartphone-based device for its ability to image and record results, which is good for tracking bacterial contamination along the entire food chain.

2. EXPERIMENTAL SECTION

2.1. Materials.

Pluronic F127, potassium tetrachloroplatinate(II) (K_2PtCl_4), sodium tetrachloropalladate(II) (Na_2PdCl_4), hydrochloric acid (HCl), ascorbic acid, potassium carbonate (K_2CO_3), acetone, sucrose, HRP, hydrogen peroxide (H_2O_2), 3,3′,5,5′-tetramethylbenzidine (TMB), Tween-20, sucrose, phosphate-buffered saline (1× PBS, pH 7.4, 0.01 M), and bovine serum albumin (BSA) were purchased from Sigma-Aldrich (St. Louis, MO). Mouse anti-*S.* Enteritidis monoclonal antibody, mouse anti-*E. coli* O157:H7 monoclonal antibody, and goat antimouse IgG antibody were obtained from Abcam Inc. (Cambridge, MA). Goat anti-*S.* Enteritidis polyclonal antibody and goat anti-*E. coli* O157:H7 polyclonal antibody were purchased from KPL Inc. (Gaithersburg, MD). Nitrocellulose membrane, glass fiber, backing cards, and an absorbent pad were purchased from Millipore (Billerica, MA).

2.2. Preparation and Inactivation of Bacteria Samples.

S. Enteritidis PT30 was from American Tissue Culture Collection (ATCC, Manassas, VA). *E. coli* O157:H7 EDL933 was obtained from the STEC center at Michigan State University. *Listeria innocua* (NRRL B-33197) was obtained from USDA ARS culture collection. *Staphylococcus aureus* (91.48) was a mastitic isolate from the cow mastitis case.[32] These strains were maintained at −80 °C in trypticase soy broth (Becton, Dickinson and Company, Sparks, MD) supplied with 0.6% yeast extract (Fisher Scientific, Fair Lawn, NJ) (TSBYE) and 15% (v/v) glycerol. Bacteria were first activated in TSBYE at 37 °C for 8 h statically; then, 1:1000 were transferred to TSBYE for the second activation at 37 °C statically for additional 14 h. The twice activated culture was washed once with phosphate-buffered saline (PBS, pH 7.4) and resuspended in sterile PBS. The resulting bacterial suspension was used as a live cell in the recovery experiment of spiked food samples. For inactivated bacterial cell preparation, the above prepared bacterial suspension was heat-inactivated in boiling water for 30 min, followed by addition of formalin (J.T. Baker, Phillipsburg, NJ) to a final concentration of 0.5% (v/v). Inactivated bacterial cells were used to optimize the conditions and evaluate the performance of the developed dual LFIA.

2.3. Preparation of Mesoporous Pd@Pt Nanoparticles.

Mesoporous Pd@Pt nanoparticles were synthesized according to our previous published method with modification.[33] Briefly, 20 mg of Pluronic F127 was ultrasonically dissolved in aqueous solution containing 1.8 mL of K_2PtCl_4 (20 mM), 0.2 mL of Na_2PdCl_4 (20 mM) solution, and 44 μL of HCl (6 M). The mixture was processed by an ultrasonic method for 4 h after adding 2.0 mL of ascorbic acid (100 mM). The final product was centrifuged at 10 000 rpm for 5 min, the resulting pellet was washed with 4 mL of acetone three times. After freeze-drying and resuspending in 5 mL of water, the concentration of the as-synthesized Pd@Pt nanoparticles was 2 mg/mL.

2.4. Preparation of Antibody-Modified Pd@Pt Nanoparticle Conjugations.

Antibody-modified Pd@Pt nanoparticle conjugations were prepared by a modified method according to the literature.[34] First, the pH of the Pd@Pt nanoparticles solution (2 mg/mL)

was adjusted to 8.2–8.5 by adding 0.02 M K_2CO_3. Then, 5 μL of mouse anti-*S.* Enteritidis monoclonal antibody (1 mg/mL) or mouse anti-*E. coli* O157:H7 monoclonal antibody (1 mg/mL) was added into the 1 mL of adjusted Pd@Pt nanoparticles solution. After incubation for 60 min at room temperature, 10.0 wt % BSA was added to the mixture, followed by 30 min of incubation. After that, the mixture was centrifuged at 10 000 rpm for 20 min and washed with 1× PBS containing 1% BSA twice. Finally, the prepared antibody-modified Pd@Pt nanoparticle conjugations were collected and suspended in 100 μL of PBS buffer containing 2% BSA and 3% sucrose.

2.5. Preparation of Dual Lateral Flow Immunoassays.

The dual LFIA consisted of a triangle-shaped sample pad (9 mm × 20 mm), two conjugate pads (4 mm × 5 mm), two nitrocellulose membranes (4 mm × 30 mm), two absorbent pads (4 mm × 15 mm), and an interoperable backing (Scheme 1A). The sample pad was made from glass fiber and saturated with 1× PBS containing 1% BSA and 0.25% Tween-20 and then dried overnight at room temperature. Two test lines (S and E) and two control lines were prepared by dispensing 30 μL of goat anti-*Salmonella* polyclonal antibody (or goat anti-*E. coli* O157:H7 polyclonal antibody) solution (1.0 mg/mL) and 30 μL of goat antimouse IgG antibody solution (0.5 mg/mL) at different locations on the nitrocellulose membrane using a BioDot BioJet BJQ 3000 dispenser (Irvine, CA). The distance between the lines was approximately 1 cm. The nitrocellulose membranes were then dried overnight at 37 °C and stored at 4 °C. Then, 2.5 μL of each antibody-modified Pd@Pt nanoparticle conjugation (20 mg/mL) was precoated on the corresponding conjugate pads after performing a short-timed ultrasound. These pads were assembled on the backing with an overlap of approximately 2–3 mm. Single LFIAs were cut at a width of 4 mm using a BioDot Paper Cutter module CM4000 (Irvine, CA). Finally, two LFIAs with different test lines (S or E) were assembled together on the triangle-shaped sample pad. The assembled dual LFIA was either used immediately or stored under dry conditions at room temperature for further tests.

2.6. Fabrication of 3D-Printed Smartphone Accessory Device.

The smartphone accessory was designed with computer-aided design software SolidWorks (Dassault System, MA) based on Apple iPhone 5s (Apple Inc., CA). The iPhone 5s was equipped with a rear iSight 8 megapixel sensor, 1.5 μm pixels, and an f/2.2 aperture. A commercial fused filament deposition 3D printer (Einstart S, Shining 3D, Hangzhou, Zhejiang, China) was used for the rapid prototyping of the smartphone accessory. A black poly(lactic acid) (PLA) filament was used for the smartphone holder to minimize light leakage, and a white PLA filament was used to utilize the ambient light for sample illumination (Scheme 1C). A plano convex lens with a diameter of 10 mm is placed in front of a camera to shorten the imaging distance and thus reduce the overall size of the device. The lens is fixed in a 3D-printed tube with three plastic threaded screws positioned in a triangular form to prevent lens movement from the operation vibration. The dual LFIA minicartridge was fabricated by laser cutting and engraving (trotec Speedy 300, Trotect., MI) a poly(methyl methacrylate) (PMMA) board for consistent and tight fit with the smartphone accessory. The smartphone accessory has a dimension of 73 mm (*L*), 35 mm (*W*), and 20 mm (*H*) and a weight of a total of 45.9 g, excluding the smartphone and

the dual LFIA cartridge. An app was used to control the image capture parameters (ISO 200, exposure time of 1660.035 s, redGain: 2.77828, greenGain: 3.36689, and blueGain: 2.68713).

2.7. Assay Procedure.

In a typical test, a dual LFIA was preset in the minicartridge. Afterward, 90 μL of running buffer (1× PBS containing 0.25% Tween-20) was mixed with 10 μL of sample, then loaded to the triangle-like sample pad of dual LFIA and migrated up due to capillary force. After 1 min, the black lines appeared visually. After adding 1 μL of TMB solution on test lines, the final blue signals were observed on the lines of dual LFIA within 10 min. When *S.* Enteritidis and *E. coli* O157:H7 are present in the sample, they will bind to their own antibody-modified Pd@Pt nanoparticle conjugations and then combine with capture antibodies on the test line-S and test line-E, thereby forming two visible blue lines (Figure S1A). If only *S.* Enteritidis or *E. coli* O157:H7 is present in the sample, only one blue line can be formed (Figured S1B,C). When a negative control sample was applied onto the sample pad, no blue line was observed in the test lines (Figure S1D). The control line indicated that the assay worked properly and the signal at the test line is reliable. Meanwhile, the minicartridge was inserted into the 3D-printed smartphone reader to obtain the results. An iPhone 5S (Apple) with an 8 megapixel (8 MP) camera was used. The image analysis software, ImageJ (NIH, MD), can provide a graphical readout of the peak area.

2.8. Detection of Live Bacteria-Contaminated Milk and Ice Cream Samples.

To demonstrate the proof-of-concept and its potential application in food samples, milk and ice cream samples were spiked with a known number of live bacteria and then detected using the proposed dual LFIA. Two percent low fat milk and double strawberry light ice cream samples were purchased from Walmart supermarket (Pullman, WA). Only negative samples were selected for being spiked by live bacteria. Milk (10 mL/g) and ice cream were added to 90 mL of sterile PBS from which we prepared samples in the final concentrations of bacteria at 1×10^4 and 1×10^5 cfu/mL. Then, the spiked samples were evaluated using the same above-mentioned condition and the recovery (%) of bacteria from milk and ice cream samples was obtained according to the above calibration curve results.

2.9. Characterization.

The morphologies of the nanomaterial were characterized by transmission electron microscopy (TEM) using a Philips CM200 UT (Field Emission Instruments) at an accelerating voltage of 40 kV. The ζ potential was measured using a zeta potential analyzer (Brookhaven Instruments Co.). Fourier transform infrared (FTIR) spectra were recorded in the range of 400–4000 cm^{-1} with 0.5–4 cm^{-1} resolution using a Tensor 27 FTIR spectrophotometer. All of the measurements were performed at room temperature.

3. RESULTS AND DISCUSSION

3.1. Characterization.

To investigate the morphology of Pd@Pt nanoparticles, transmission electron microscope (TEM) images were collected. As shown in Figure 1A–C, the crystal growth was happened

on the surface of Pd nanocrystals and on tips of the active branches[35] and the as-synthesized Pd@Pt nanoparticle size was approximately 35 nm. To verify the successful conjugation of antibody, we measured ζ potential and FTIR spectra of Pd@Pt nanoparticles before and after modification. As shown in Table S1, the ζ potential decreased from −40.6 to −32.5 mV for *S.* Enteritidis antibody conjugations and from −40.6 to −33.5 mV for *E. coli* O157:H7 antibody conjugations. As shown in Figure S2, a small peak around 1550 cm^{-1} corresponding to amino groups was observed after antibody modification in the FTIR spectra,[36] which further confirmed antibody functionalization successfully.

The function of antibody-modified Pd@Pt nanoparticle conjugation is a critical factor for dual LFIA. Antibody-modified Pd@Pt nanoparticle conjugation is composed of two parts: anti-*S.* Enteritidis antibodies (or anti-*E. coli* O157:H7 antibodies) with recognition function and Pd@Pt nanoparticles with catalytic activity. First, we test whether the proposed antibodies could recognize *S.* Enteritidis and *E. coli* O157:H7. As shown in Figure 1D–G, TEM images confirmed that *S.* Enteritidis and *E. coli* O157:H7 could be captured by antibody-conjugated Pd@Pt nanoparticles. Then, we use antibody-conjugated Pd@Pt nanoparticles to catalyze the oxidation of TMB. The results demonstrated that the antibody-modified Pd@Pt nanoparticle conjugation had similar catalytic activity with the solution of HRP and unmodified Pd@Pt nanoparticles (Figure S3). Together, these results indicated that antibody-conjugated Pd@Pt nanoparticles possessed the dual functions (capturing bacteria and catalytic activity).

3.2. Mechanism.

To achieve double capacity of lateral flow immunoassays, we banded single plexes together in parallel instead of adding two test lines in a single LFIA (Scheme 1A). The design of such dual-detection systems was based on careful consideration of cross-reactivity and the limitation of Washburn's theory.[24,37] The proposed dual LFIAs could provide the same sensitivity of multiplexed detection as that of individual single LFIA detection. To further improve the sensitivity of the dual LFIA, we employed Pd@Pt nanoparticles instead of AuNPs as signal amplification (Scheme 1B). The Pd@Pt nanoparticles modified by antibodies owned dual functions: recognition and signal amplification. Owing to the intrinsic peroxidase-like catalytic activity, the antibody-modified Pd@Pt nanoparticle conjugations can generate stronger blue color in the presence of TMB and H_2O_2.[38,39] The enhancement of signals on the two test lines are critical for the detection of low level of pathogens. To provide a field-portable, cost-effective platform with high sensitivity, the smartphone-based device was developed to image and record results. The device consists of three parts, a 3D-printed cover, holder, and smartphone accessory, resulting in an integrated tool (Scheme 1C). Together, the proposed assay is portable and sensitive without any complex sample pre-enrichment and specialized instruments, making it a valuable detection tool for foodborne pathogens.

3.3. Optimization.

To acquire sensitive detection with enhanced signal, we compared the catalytic capability of different-sized Pd@Pt nanoparticles first, which were synthesized by adding various amounts of surfactants, Pluronic F127 (10, 20, and 30 mg) in solution. As shown in

Figure S4, the as-synthesized Pd@Pt nanoparticle size was approximately 40 nm for 10 mg surfactants, approximately 35 nm for 20 mg surfactants, and approximately 15 nm for 30 mg surfactants. Insufficient gametes (10 mg) lead to larger particles and less surface area, which results in weaker catalytic capacity than that of 20 mg of gametes. Excessive gametes (30 mg) led to smaller particles and fewer branches, which were also not suitable as signal elements in our system due to weak catalytic capacity. After optimization, the amount of Pluronic F127 used to prepare Pd@Pt nanoparticles was selected to be 20 mg in the following experiments. To achieve the best performance of the dual LFIA, the reaction system were further optimized. The amount of antibody-modified Pd@Pt nanoparticle conjugations on the conjugate pad could affect the hybridization efficiency between bacteria and corresponding antibody and thus the performance of dual LFIA. As seen from Figure 2A, the peak area increased up to 2.5 μL and then decreased at 3.0 μL. The peak area loss occurred at a high concentration probably due to stereo hindrance between bacteria and antibody-modified Pd@Pt nanoparticle conjugations. Therefore, 2.5 μL of antibody-modified Pd@Pt nanoparticle conjugations was the optimal amount and was used in the further experiments. Figure 2B showed the results for the time after adding TMB solution. The peak area increased as the reaction time increased until 12 min and decreased as the reaction time increased after 12 min. No significant difference was observed in the peak area for assays between the reaction times of 8 and 12 min. A hybridization time of 10 min was selected for all subsequent tests. Running buffer also plays an important role, as it can minimize nonspecific adsorption and increase the sensitivity of the dual LFIA. As shown in Figure 2C, with increasing BSA, the corresponding response decreased significantly, especially when adding TMB solution. BSA-free 1× PBS was found to be the optimal running buffer, whereas 1% of BSA was added in the solution to prepare the sample pad. Figure 2D shows that the responses remained almost the same with varying amounts of Tween-20 in the running buffer with TMB solution. However, in the condition of the signal without TMB enhancement, the best result was obtained with 0.25% Tween-20, which was used as the optimal running buffer in subsequent detections.

3.4. Performance for Pathogen Detection.

The sensitivities of optimized dual LFIA were further estimated using sample solutions containing various concentrations of targets under the optimized experimental conditions. Figure 3A displays the typical photo image of the dual LFIAs with different bacterial concentrations ranging from 0 to 10^8 cfu/mL. The detection limit of *S.* Enteritidis and *E. coli* O157:H7 without TMB and H_2O_2 were both approximately 10^6 cfu/mL (Figure 3B,C), which was dramatically improved after adding TMB and H_2O_2 (Figure 3D). The blue band in the dual LFIA test zone was observed with as low as 10 cfu/mL of *S.* Enteritidis and *E. coli* O157:H7 without any pre-enrichment (Figure 3D), which was 100-fold more sensitive than previously published AuNP-based LFIAs and similar to reported HRP-enhanced LFIAs (Table 1). Quantitative detection was performed by recording the peak areas of the two test lines (S and E) (Figure 3E). The resulting calibration curves were exponential for both pathogens over the 10–10^7 cfu/mL range (Figure 3F). The LODs based on 3.3 × standard deviation (SD)/slope of the calibration curve were calculated to be ~20 cfu/mL for *S.* Enteritidis and ~34 cfu/mL for *E. coli* O157:H7, indicating that approximately 2–3 cfus present in 100 μL of the sample can be quantified using this dual LFIA. These

results well demonstrate the sensitive performance of our assay for simultaneous detection of two pathogens, which is contributed by the peroxidase-like catalytic activity of the Pd@Pt nanoparticles for signal enhancement and the parallel design of dual detection for noninterference.

The specificity of dual LFIA was further evaluated with other bacteria and PBS. We detected a mixture of *S.* Enteritidis and *E. coli* O157:H7 as well as *S.* Enteritidis, *E. coli* O157:H7, a mixture of *S.* Enteritidis and *Listeria*, a mixture of *E. coli* O157:H7 and *S. aureus*, and *Listeria* and *S. aureus* by dual LFIAs. No distinct blue band was observed on the test lines of dual LFIAs in the samples in absence of corresponding bacteria, as expected (Figure S5). No cross-reactivity with other bacteria was confirmed by *Listeria* and *S. aureus* (Figure S5). In addition, no signal was observed in the PBS control test, indicating negligible nonspecific adsorption of the optimized dual LFIA.

The stability test was performed by storing the dual LFIA at room temperature during the recent 30 day period using the same batch of strips. Dual LFIAs were stored in Ziploc bags under dark and dry conditions and intermittently measured (every 10 days). During the stability examination, their responses did not change significantly and the intensities of the test lines on the dual LFIA for 10^4 cfu/mL *S.* Enteritidis and 10^4 cfu/mL *E. coli* O157:H7 showed the coefficient of variation as less than 7% compared to that obtained with the newly prepared dual LFIA (data not shown). Thus, the dual LFIA was still usable after 30 days of storage at room temperature, indicating that the dual LFIA approach has a good stability.

To demonstrate the potential application of the dual LFIA in food samples, the device was used to detect live *S.* Enteritidis and *E. coli* O157:H7 spiked in milk or ice cream samples from 10^2 to 10^5 cfu/mL. The estimated recoveries of the dual LFIA range from 91.44 to 117.00% (Table 2), which clearly indicated that the developed method is capable of detecting live *S.* Enteritidis and *E. coli* O157:H7 in real food samples.

4. CONCLUSIONS

In summary, this is the first report of quantitative dual LFIA for simultaneously detecting two pathogens, employing nanozyme as the signal reporter and smartphone as the result recorder. By using mesoporous Pd@Pt nanoparticles for signal enhancement and the parallel design of dual detection, the LODs were calculated to be ~20 cfu/mL for *S.* Enteritidis and ~34 cfu/mL for *E. coli* O157:H7. The estimated recoveries of the dual LFIA range from 91.44 to 109.56% (blow 10^5 cfu/mL), which indicated that the developed method is capable of detecting bacteria in food samples. The smartphone was used to image and record results, which is good for tracking bacterial contamination along the entire food chain. Compared with conventional LFIAs, the current approach is much more sensitive and portable, avoiding the use of complex sample pre-enrichment and specialized instruments. Although the current format requires loading of TMB solutions during the experiment, this process can be further simplified by sealing them in blister packs and bursting them open prior to use. Such integration is expected to further simplify the assay for making it more suitable for on-site applications by a wide range of users.

Supplementary Material

Refer to Web version on PubMed Central for supplementary material.

ACKNOWLEDGMENTS

This work was supported by a WSU strartup fund and the Centers for Disease Control and Prevention/ National Institute for Occupational Safety and Health (CDC/NIOSH), Grant No. R01OH011023–01A1 and China Scholarship Council (201606350119) to N.C. Its contents are solely the responsibility of the authors and do not necessarily represent the official views of CDC.

REFERENCES

(1). Zhang Z; Zhang X; Liu B; Liu J Molecular Imprinting on Inorganic Nanozymes for Hundred-Fold Enzyme Specificity. J. Am. Chem. Soc. 2017, 139, 5412–5419. [PubMed: 28345903]

(2). Wang Q; Zhang X; Huang L; Zhang Z; Dong S One-Pot Synthesis of Fe3O4 Nanoparticle Loaded 3d Porous Graphene Nanocomposites with Enhanced Nanozyme Activity for Glucose Detection. ACS Appl. Mater. Interfaces 2017, 9, 7465–7471. [PubMed: 28125774]

(3). Sun A; Mu L; Hu X Graphene Oxide Quantum Dots as Novel Nanozymes for Alcohol Intoxication. ACS Appl. Mater. Interfaces 2017, 9, 12241–12252. [PubMed: 28322544]

(4). Nagvenkar AP; Gedanken A Cu0. 89zn0. 11o, a New Peroxidase-Mimicking Nanozyme with High Sensitivity for Glucose and Antioxidant Detection. ACS Appl. Mater. Interfaces 2016, 8, 22301–22308. [PubMed: 27503256]

(5). Nasrabadi HT; Abbasi E; Davaran S; Kouhi M; Akbarzadeh A Bimetallic Nanoparticles: Preparation, Properties, and Biomedical Applications. Artif. Cells, Nanomed., Biotechnol. 2016, 44, 376–380. [PubMed: 25203939]

(6). Yuan C-X; Fan Y-R; Guo H-X; Zhang J-X; Wang Y-L; Shan D-L; Lu X-Q A New Electrochemical Sensor of Nitro Aromatic Compound Based on Three-Dimensional Porous Pd@Pt Nanoparticles Supported by Graphene–Multiwalled Carbon Nanotube Composite. Biosens. Bioelectron. 2014, 58, 85–91. [PubMed: 24632133]

(7). Hossain M; Park JY Amperometric Glucose Biosensor Based on Pt-Pd Nanoparticles Supported by Reduced Graphene Oxide and Integrated with Glucose Oxidase. Electroanalysis 2014, 26, 940–951.

(8). Wang Y; Qin Z; Boulware DR; Pritt BS; Sloan LM; González IJ; Bell D; Rees-Channer RR; Chiodini P; Chan WC; Bischof JC Thermal Contrast Amplification Reader Yielding 8-Fold Analytical Improvement for Disease Detection with Lateral Flow Assays. Anal. Chem. 2016, 88, 11774–11782. [PubMed: 27750420]

(9). Scallan E; Hoekstra R; Mahon B; Jones T; Griffin P An Assessment of the Human Health Impact of Seven Leading Foodborne Pathogens in the United States Using Disability Adjusted Life Years. Epidemiol. Infect. 2015, 143, 2795–2804. [PubMed: 25633631]

(10). Kirk MD; Pires SM; Black RE; Caipo M; Crump JA; Devleesschauwer B; Döpfer D; Fazil A; Fischer-Walker CL; Hald T World Health Organization Estimates of the Global and Regional Disease Burden of 22 Foodborne Bacterial, Protozoal, and Viral Diseases, 2010: A Data Synthesis. PLoS Med. 2015, 12, No. e1001921. [PubMed: 26633831]

(11). Lipkin WI The Changing Face of Pathogen Discovery and Surveillance. Nat. Rev. Microbiol. 2013, 11, 133–141. [PubMed: 23268232]

(12). Singh J; Sharma S; Nara S Evaluation of Gold Nanoparticle Based Lateral Flow Assays for Diagnosis of Enterobacteriaceae Members in Food and Water. Food Chem. 2015, 170, 470–483. [PubMed: 25306373]

(13). Geissler M; Clime L; Hoa XD; Morton KJ; Hêbert H; Poncelet L; Mounier M; Deschênes M. n.; Gauthier ME; Huszczynski G; et al. Microfluidic Integration of a Cloth-Based Hybridization Array System (Chas) for Rapid, Colorimetric Detection of Enterohemorrhagic Escherichia coli (Ehec) Using an Articulated, Centrifugal Platform. Anal. Chem. 2015, 87, 10565–10572. [PubMed: 26416260]

(14). Zhang Y; Tan C; Fei R; Liu X; Zhou Y; Chen J; Chen H; Zhou R; Hu Y Sensitive Chemiluminescence Immunoassay for *E. coli* O157: H7 Detection with Signal Dual-Amplification Using Glucose Oxidase and Laccase. Anal. Chem. 2014, 86, 1115–1122. [PubMed: 24405233]

(15). Verbarg J; Plath WD; Shriver-Lake LC; Howell PB Jr.; Erickson JS; Golden JP; Ligler FS Catch and Release: Integrated System for Multiplexed Detection of Bacteria. Anal. Chem. 2013, 85, 4944–4950. [PubMed: 23631439]

(16). Posthuma-Trumpie GA; Korf J; van Amerongen A Lateral Flow (Immuno) Assay: Its Strengths, Weaknesses, Opportunities and Threats. A Literature Survey. Anal. Bioanal. Chem. 2009, 393, 569–582. [PubMed: 18696055]

(17). Ngom B; Guo Y; Wang X; Bi D Development and Application of Lateral Flow Test Strip Technology for Detection of Infectious Agents and Chemical Contaminants: A Review. Anal. Bioanal. Chem. 2010, 397, 1113–1135. [PubMed: 20422164]

(18). Hassan A-R; de la Escosura-Muñiz A; Merkoçi A Highly Sensitive and Rapid Determination of *Escherichia coli* O157: H7 in Minced Beef and Water Using Electrocatalytic Gold Nanoparticle Tags. Biosens. Bioelectron. 2015, 67, 511–515. [PubMed: 25241123]

(19). Qi H; Zhong Z; Zhou H-X; Deng C-Y; Zhu H; Li J-F; Wang X-L; Li F-R A Rapid and Highly Sensitive Protocol for the Detection of Escherichia coli O157: H7 Based on Immunochromatography Assay Combined with the Enrichment Technique of Immunomagnetic Nanoparticles. Int. J. Nanomed. 2011, 6, 3033.

(20). Xi C; Xiong Q-R; Xiong Y-H; Shan S; Wei-Hua L Establishing of a Method Combined Immunomagnetic Separation with Colloidal Gold Lateral Flow Assay and Its Application in Rapid Detection of *Escherichia coli* O157: H7. Chin. J. Anal. Chem. 2013, 41, 1812–1816.

(21). Song C; Liu C; Wu S; Li H; Guo H; Yang B; Qiu S; Li J; Liu L; Zeng H; et al. Development of a Lateral Flow Colloidal Gold Immunoassay Strip for the Simultaneous Detection of Shigella boydii and Escherichia coli O157: H7 in Bread, Milk and Jelly Samples. Food Control 2016, 59, 345–351.

(22). Wang J; Katani R; Li L; Hegde N; Roberts EL; Kapur V; DebRoy C Rapid Detection of Escherichia coli O157 and Shiga Toxins by Lateral Flow Immunoassays. Toxins 2016, 8, 92. [PubMed: 27023604]

(23). Fenton EM; Mascarenas MR; López GP; Sibbett SS Multiplex Lateral-Flow Test Strips Fabricated by Two-Dimensional Shaping. ACS Appl. Mater. Interfaces 2009, 1, 124–129. [PubMed: 20355763]

(24). Li J; Macdonald J Multiplexed Lateral Flow Biosensors: Technological Advances for Radically Improving Point-of-Care Diagnoses. Biosens. Bioelectron. 2016, 83, 177–192. [PubMed: 27125840]

(25). Jokerst JC; Adkins JA; Bisha B; Mentele MM; Goodridge LD; Henry CS Development of a Paper-Based Analytical Device for Colorimetric Detection of Select Foodborne Pathogens. Anal. Chem. 2012, 84, 2900–2907. [PubMed: 22320200]

(26). Wen W; Yan X; Zhu C; Du D; Lin Y Recent advances in electrochemical immunosensors. Anal. Chem. 2017, 89, 138–156. [PubMed: 28105820]

(27). Wei Q; Nagi R; Sadeghi K; Feng S; Yan E; Ki SJ; Caire R; Tseng D; Ozcan A Detection and Spatial Mapping of Mercury Contamination in Water Samples Using a Smart-Phone. ACS Nano 2014, 8, 1121–1129. [PubMed: 24437470]

(28). Yang M; Sun R; Wang S; Smith JN; Timchal C; Li L; Lin Y; Du DA 3D-Printed, Portable, Optical-Sensing Platform for Smartphones Capable of Detecting the Herbicide 2, 4-Dichlorophenoxyacetic Acid. Anal. Chem. 2017, 89, 9339–9346. [PubMed: 28727917]

(29). You DJ; San Park T; Yoon J-Y Cell-Phone-Based Measurement of Tsh Using Mie Scatter Optimized Lateral Flow Assays. Biosens. Bioelectron. 2013, 40, 180–185. [PubMed: 22863118]

(30). Cooper DC Mobile Image Ratiometry for the Detection of Botrytis Cinerea (Gray Mold). Nat. Precedings 2012, DOI: 10.1038/npre.2012.6989.1.

(31). Lee S; Kim G; Moon J Development of a Smartphone-Based Reading System for Lateral Flow Immunoassay. J. Nanosci. Nanotechnol. 2014, 14, 8453–8457. [PubMed: 25958545]

(32). Roberson JR; Fox LK; Hancock DD; Besser TE Evaluation of Methods for Differentiation of Coagulase-Positive Staphylococci. J. Clin. Microbiol. 1992, 30, 3217–3219. [PubMed: 1452705]

(33). Ataee-Esfahani H; Imura M; Yamauchi Y All-Metal Mesoporous Nanocolloids: Solution-Phase Synthesis of Core-Shell Pd@Pt Nanoparticles with a Designed Concave Surface. Angew. Chem., Int. Ed. 2013, 52, 13611–13615.

(34). Jiang T; Song Y; Du D; Liu X; Lin Y Detection of P53 Protein Based on Mesoporous Pd@Pt Nanoparticles with Enhanced Peroxidase-Like Catalysis. ACS Sens. 2016, 1, 717–724.

(35). Wu H; Mei S; Cao X; Zheng J; Lin M; Tang J; Ren F; Du Y; Pan Y; Gu H Facile Synthesis of Pt/Pd Nanodendrites for the Direct Oxidation of Methanol. Nanotechnology 2014, 25, No. 195702. [PubMed: 24762712]

(36). Hu J; Wei T; Sun S; Zhao A; Xu C Effects of Cigarette Smoke Condensate on the Production and Characterization of Exopolysaccharides by Bifidobacterium. An. Acad. Bras. Cienc. 2015, 87, 997–1005. [PubMed: 26062117]

(37). Cheng N; Shang Y; Xu Y; Zhang L; Luo Y; Huang K; Xu W On-Site Detection of Stacked Genetically Modified Soybean Based on Event-Specific Tm-Lamp and a Dnazyme-Lateral Flow Biosensor. Biosens. Bioelectron. 2017, 91, 408–416. [PubMed: 28064126]

(38). Wang J; Gu H Novel Metal Nanomaterials and Their Catalytic Applications. Molecules 2015, 20, 17070–17092. [PubMed: 26393550]

(39). Chen X; Su B; Cai Z; Chen X; Oyama M Ptpd Nanodendrites Supported on Graphene Nanosheets: A Peroxidase-Like Catalyst for Colorimetric Detection of H_2O_2. Sens. Actuators, B 2014, 201, 286–292.

(40). Luo K; Hu L; Guo Q; Wu C; Wu S; Liu D; Xiong Y; Lai W Comparison of 4 Label-Based Immunochromatographic Assays for the Detection of *Escherichia coli* O157: H7 in Milk. J. Dairy Sci. 2017, 100, 5176. [PubMed: 28457546]

(41). Chen M; Yu Z; Liu D; Peng T; Liu K; Wang S; Xiong Y; Wei H; Xu H; Lai W Dual Gold Nanoparticle Lateflow Immunoassay for Sensitive Detection of *Escherichia coli* O157: H7. Anal. Chim. Acta 2015, 876, 71–76. [PubMed: 25998460]

(42). Xia S; Yu Z; Liu D; Xu C; Lai W Developing a Novel Immunochromatographic Test Strip with Gold Magnetic Bifunctional Nanobeads (Gmbn) for Efficient Detection of Salmonella choleraesuis in Milk. Food Control 2016, 59, 507–512.

(43). Hwang J; Kwon D; Lee S; Jeon S Detection of Salmonella Bacteria in Milk Using Gold-Coated Magnetic Nanoparticle Clusters and Lateral Flow Filters. RSC Adv. 2016, 6, 48445–48448.

(44). Singh J; Sharma S; Nara S Nanogold Based Lateral Flow Assay for the Detection of Salmonella typhi in Environmental Water Samples. Anal. Methods 2015, 7, 9281–9288.

(45). Wang W; Liu L; Song S; Xu L; Kuang H; Zhu J; Xu C Gold Nanoparticle-Based Strip Sensor for Multiple Detection of Twelve Salmonella Strains with a Genus-Specific Lipopolysaccharide Antibody. Sci. China Mater. 2016, 59, 665–674.

(46). Park S; Kim H; Paek S-H; Hong JW; Kim Y-K Enzyme-Linked Immuno-Strip Biosensor to Detect Escherichia coli O157: H7. Ultramicroscopy 2008, 108, 1348–1351. [PubMed: 18562109]

(47). Cho I-H; Bhunia A; Irudayaraj J Rapid Pathogen Detection by Lateral-Flow Immunochromatographic Assay with Gold Nanoparticle-Assisted Enzyme Signal Amplification. Int. J. Food Microbiol. 2015, 206, 60–66. [PubMed: 25955290]

(48). Ren W; Cho I-H; Zhou Z; Irudayaraj J Ultrasensitive Detection of Microbial Cells Using Magnetic Focus Enhanced Lateral Flow Sensors. Chem. Commun. 2016, 52, 4930–4933.

(49). Cho I-H; Irudayaraj J Lateral-Flow Enzyme Immunoconcentration for Rapid Detection of *Listeria monocytogenes*. Anal. Bioanal. Chem. 2013, 405, 3313–3319. [PubMed: 23354582]

(50). Park S; Kim YT; Kim Y-K Optical Enzyme-Linked Immunosorbent Assay on a Strip for Detection of Salmonella typhimurium. BioChip J. 2010, 4, 110–116.

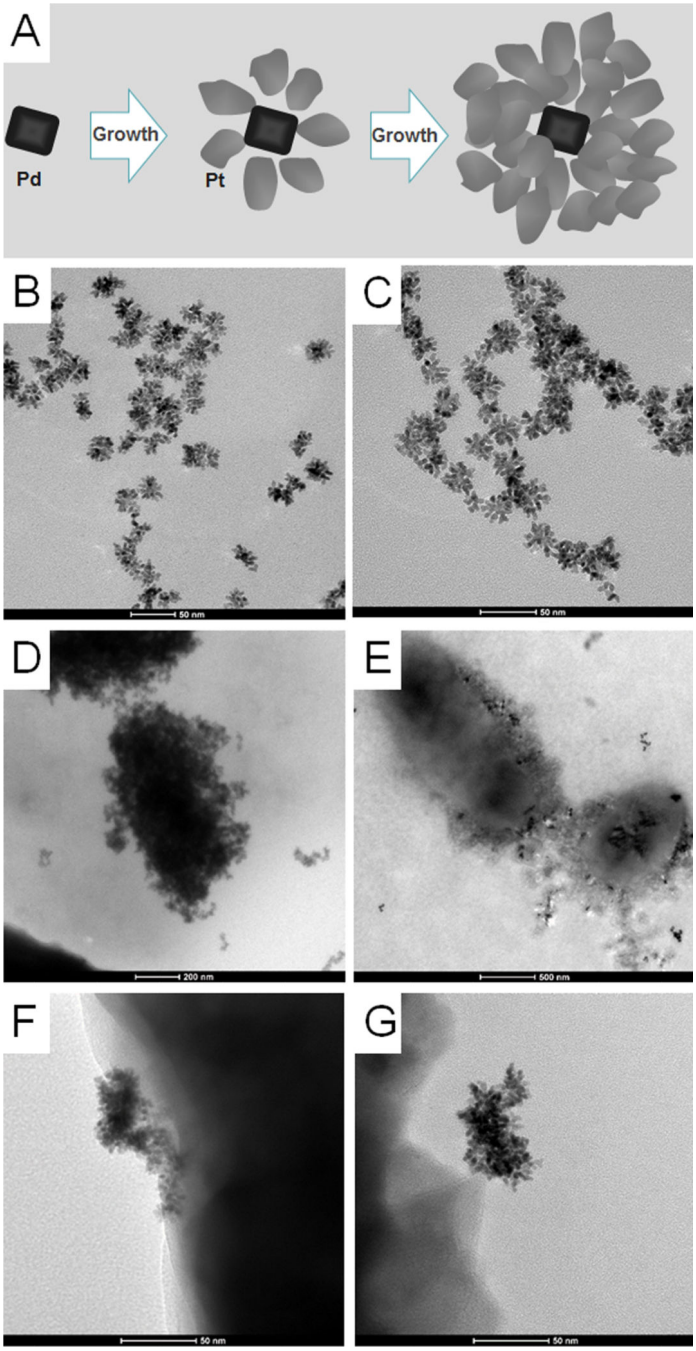

Figure 1.

Synthesis scheme and TEM imaging. (A) Schematic illustration of Pd@Pt nanoparticles formation. (B, C) TEM images of Pd@Pt nanoparticles, with a mean diameter of 35 nm. (D) TEM image of *E. coli* O157:H7 captured by antibody-modified Pd@Pt nanoparticle conjugations. (E) TEM image of *S.* Enteritidis captured by antibody-modified Pd@Pt nanoparticle conjugations. (F, G) TEM images of details for the recognition function of antibodies-modified Pd@Pt nanoparticle conjugations.

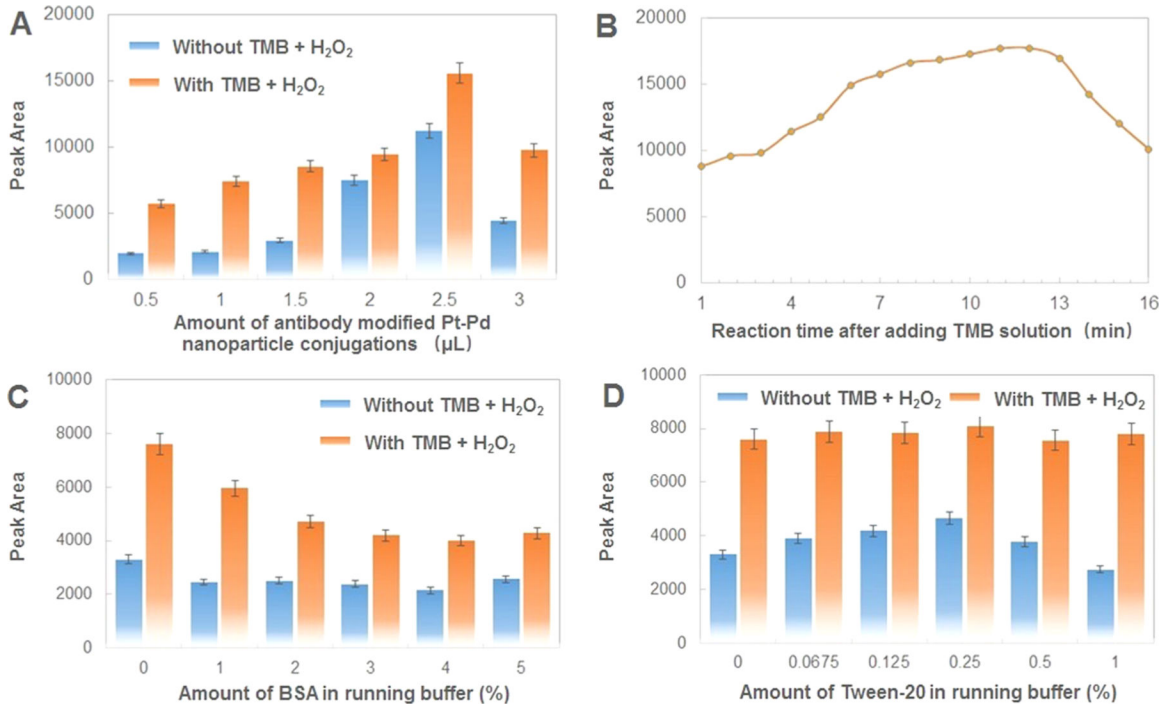

Figure 2.

Assay optimization with respect to the peak area of test lines with or without TMB and H_2O_2. (A) Effect of different amounts of antibody-modified Pd@Pt nanoparticle conjugations: 0.5, 1, 1.5, 2, 2.5, and 3 μL; concentration of target bacteria: 10^8 cfu/mL. (B) Effect of reaction time after adding TMB solution: from 1 to 16 min; concentration of target bacteria: 10^8 cfu/mL. (C) Effect of the amount of BSA in running buffer: 0, 1, 2, 3, 4, and 5%; concentration of target bacteria: 10^7 cfu/mL. (D) Effect of amount of Tween-20 in running buffer: 0, 0.0675, 0.125, 0.25, 0.5, and 1%; concentration of bacteria: 10^7 cfu/mL. Error bars indicate standard deviations of the three measurements.

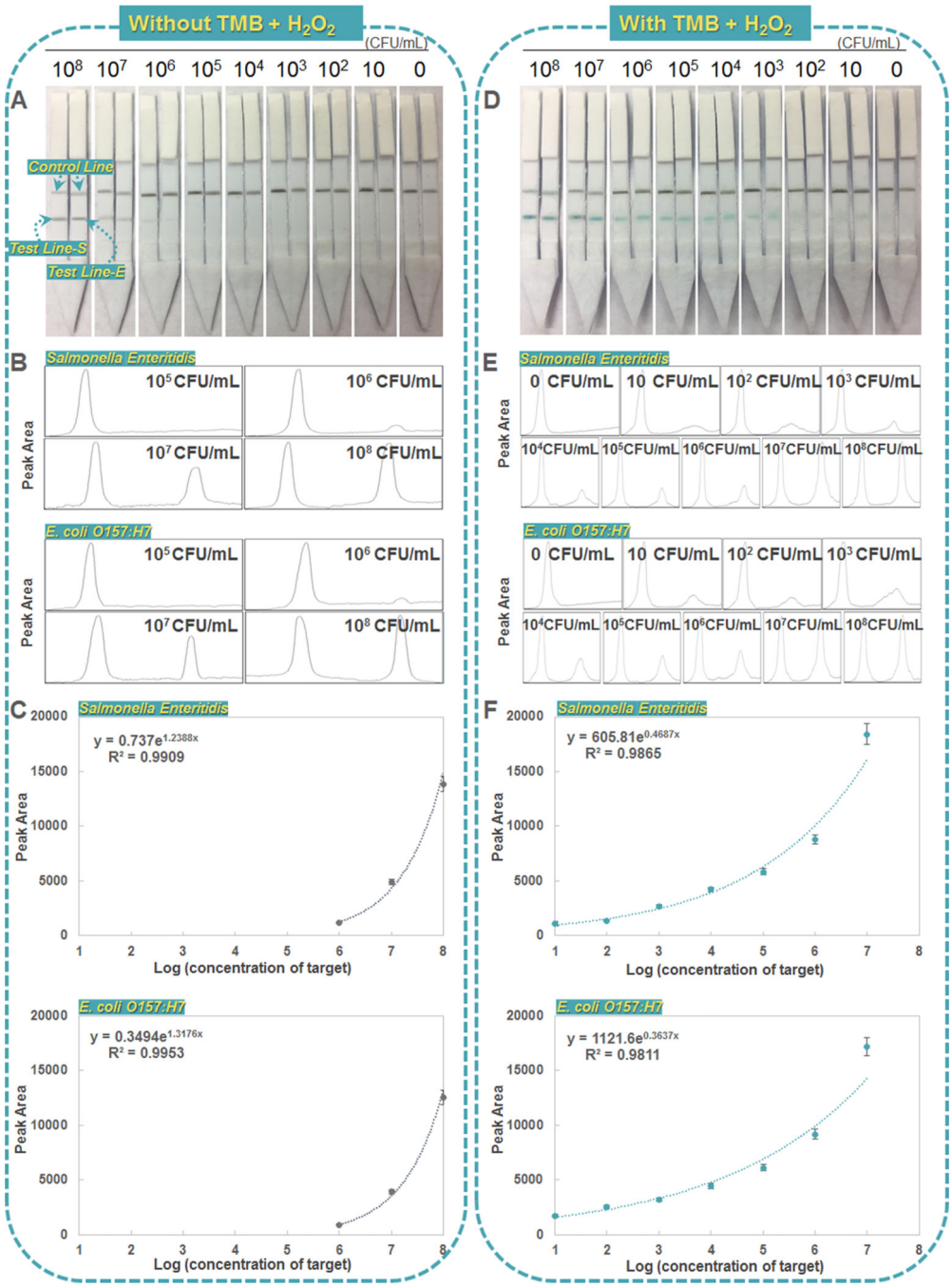

Figure 3.

Sensitivity of dual LFIA for simultaneous detection of *S.* Enteritidis and *E. coli* O157:H7. Left: dual LFIAs without TMB solution. Right: dual LFIAs with TMB solution. (A, D) Typical photo image of dual LFIAs with different bacterial concentrations ranging from 0 to 10^8 cfu/mL. (B, E) Quantitative detections were performed by plotting the peak of two test lines (S and E). (C, F) Calibration curves of peak areas of test lines vs target concentrations. Error bars indicate standard deviations of the three measurements.

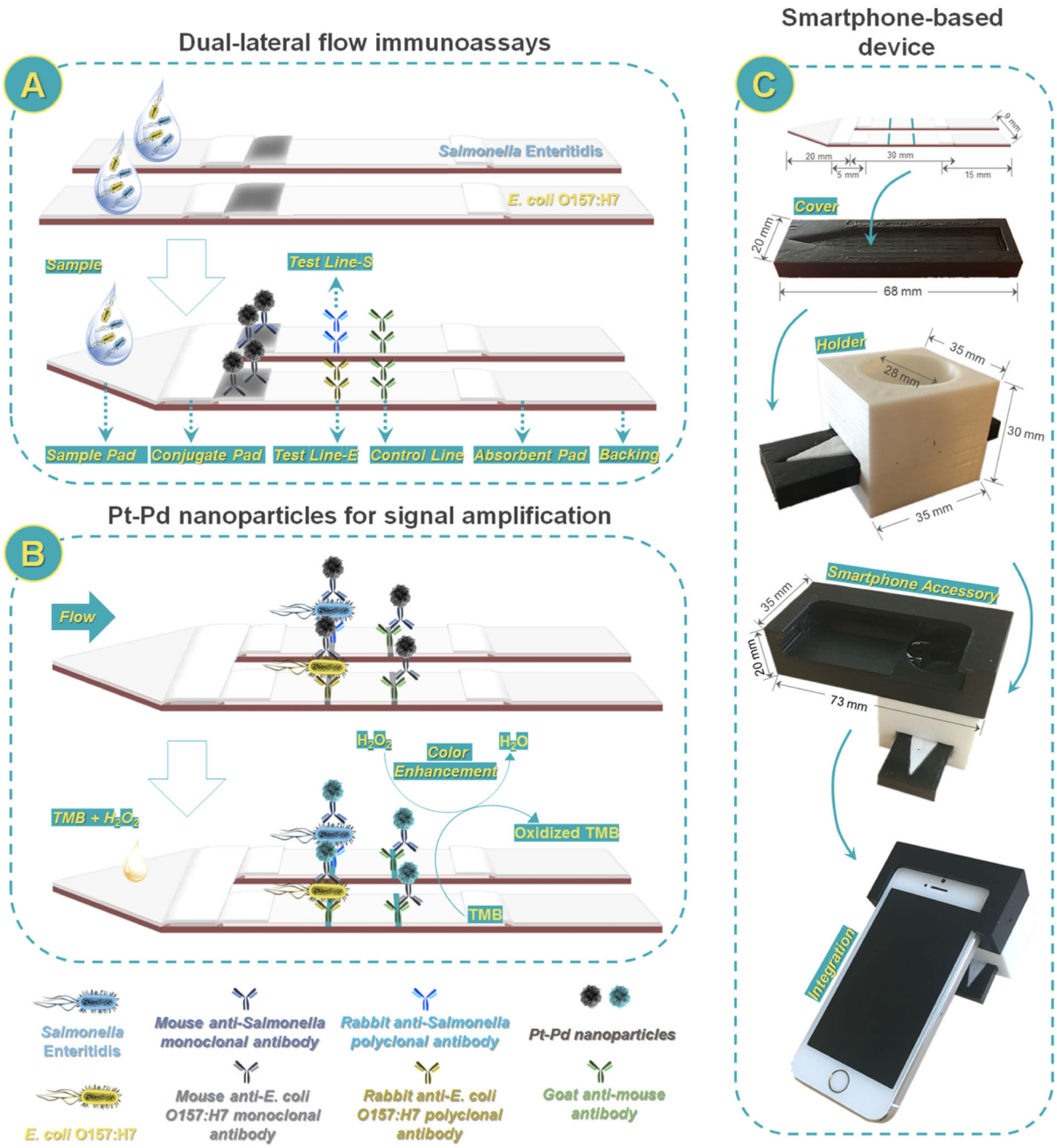

Scheme 1.

Scheme of Smartphone-Based Dual Lateral Flow Immunoassays for Simultaneous Detection of *S.* Enteritidis and *E. coli* O157:H7 Using Pd@Pt Nanoparticles as Signal Amplification[a]

[a](A) Dual lateral flow immunoassays; (B) Pd@Pt nanoparticles for signal amplification; and (C) smartphone-based device.

Table 1.

Summary of Reported LFIAs for Bacteria Detection

strategy	target	limit of detection (without enrichment) (cfu/mL)	quantitative device	simultaneous detection	ref
AuNP-based LFIAs	*E. coli* O157:H7	7.6×10^3	no	no	20
	E. coli O157:H7	10^6	no	yes (*E. coli* O157:H7 and *Shigella boydü)*	21
	E. coli O157:H7	2.5×10^4	no	no	40
	E. coli O157:H7	1.14×10^3	no	no	41
	Salmonella	5×10^5	no	no	42
	Salmonella	10^3	no	no	43
	Salmonella	10^4	no	no	44
	Salmonella	10^3	no	no	45
HRP-enhanced LFIAs	*E. coli* O157:H7	1.8×10^3	no	no	46
	E. coli O157:H7	100	no	no	47
	E. coli O157:H7	23	no	no	48
	histeria	95	no	no	49
	Salmonella	9.2×10^3	no	no	50
	Salmonella	17	no	no	48
nanozyme-based LFIA	*Salmonella* and *E. coli* O157:H7	20 and 34	yes (smartphone-based device)	yes (*S.* Enteritidis and *E. coli* O157:H7)	this work

Table 2.

Recovery Experiments of Dual LFIA for Detection of *Salmonella* and *E. coli* O157:H7 Spiked in Milk and Ice Cream

	detected (cfu/mL)		added (cfu/mL)		found (cfu/mL)		recovery (%)	
sample	***Salmonella***	***E. coli* O157:H7**	***Salmonella***	***E. coli* O157:H7**	***Salmonella***	***E. coli* O157:H7**	***Salmonella***	***E. coli* O157:H7**
milk	0	0	1×10^2	1×10^2	92	117	92.00	117.00
milk	0	0	1×10^3	1×10^3	1088	942	108.80	94.20
milk	0	0	1×10^4	1×10^4	10 664	10 396	106.64	103.96
milk	0	0	1×10^5	1×10^5	107 468	91438	107.47	91.44
ice cream	0	0	1×10^2	1×10^2	96	109	96.00	109.00
ice cream	0	0	1×10^3	1×10^3	1136	929	113.60	92.90
ice cream	0	0	1×10^4	1×10^4	10 817	10 718	108.17	107.18
ice cream	0	0	1×10^5	1×10^5	93 253	109 562	93.25	109.56